

Optimized control for high-fidelity state transmission in open systems

Yang-Yang Xie¹, Feng-Hua Ren², Arapat Ablimit¹, Xiang-Han Liang¹, Zhao-Ming Wang^{1*}

¹*College of Physics and Optoelectronic Engineering,
Ocean University of China, Qingdao 266100, People's Republic of China*

²*School of Information and Control Engineering,
Qingdao University of Technology, Qingdao 266520, People's Republic of China*

(Dated: April 24, 2023)

Quantum state transfer (QST) through spin chains has been extensively investigated. Two schemes, the coupling set for perfect state transfer (PST) or adding a leakage elimination operator (LEO) Hamiltonian have been proposed to boost the transmission fidelity. However, these ideal schemes are only suitable for closed systems and will lose their effectiveness in open ones. In this work, we invoke a well explored optimization algorithm, Adam, to expand the applicable range of PST couplings and LEO to the open systems. Our results show that although the transmission fidelity decreases with increasing system-bath coupling strength, Markovianity and temperature for both ideal and optimized cases, the fidelities obtained by the optimized schemes always outweigh the ideal cases. The enhancement becomes more bigger for a stronger bath, indicating a stronger bath provides more space for the Adam to optimize. This method will be useful for the realization of high-fidelity information transfer in the presence of environment.

I. INTRODUCTION

High-fidelity information transfer between qubits lays a firm foundation for the realization of large-scale fault-tolerant quantum computers [1]. Spin qubits interact through nearest-neighbor Heisenberg exchange coupling and constitute a one-dimensional spin chain. Bose has proposed to use a spin chain as the channel for short-distance communication [2]. Nonetheless, the transmission fidelity decreases with increasing number of spins [2, 3]. Lots of strategies for the fidelity improvement have been proposed, such as arranging the special couplings between nearest-neighbor sites for PST [4, 5], adding well-designed external fields [6–9]. QST has also been experimentally investigated in varieties of platforms, including superconducting qubit chains [10], trapped ions [11], ultracold atoms [12], semiconductor quantum dots [13, 14], etc.

Along with the above alluded ones, the proposed schemes are mainly based on ideally closed systems. When considering the environments [15, 16], normally the information processing which can be performed well in closed systems will be destroyed by the system-bath interaction. The detrimental effects of a Markovian [3] or non-Markovian [16–18] bath on the QST through spin chains have been investigated recently. The transmission fidelity is found to decrease with the increasing system-environment coupling strength, environmental characteristic frequency and temperature [16, 18]. A lot of schemes have been proposed to reduce these adverse effects, like modulating the couplings between the spins [3–5] or invoking an LEO [16, 18]. In our recent work, we investigate the almost exact state transmission in a spin chain by adding an LEO Hamiltonian [9, 16]. The LEO Hamiltonian can be

realized by a sequence of control pulses. The pulse conditions have been obtained in a closed system for almost exact QST [16]. When applying these conditions to an open system, the fidelity decreases due to the existence of the environments [16, 19].

Gradient descent is the most basic optimization algorithm [20], moving relevant parameters towards the direction minimizing a predefined cost, or loss, function but without guaranteeing a fast and stable convergence. Momentum algorithm makes progress with this problem by updating parameters according to the gradients of current and previous iterations [21]. Besides, one of the algorithms with adaptive learning rates, RMSprop [22], can modulate the learning rate on the basis of different parameters and training phases. Adaptive Moment Estimation (Adam) algorithm builds on and hence inherits the above two ones, realizing more efficient convergence behaviors, and become the most popular optimizer even in the noisy intermediate-scale quantum (NISQ) device era [23–25]. Recently we use the stochastic gradient descent or Adam algorithm to find the optimized pulses for the adiabatic speedup [26] or non-adiabatic QST [27] in a noisy environment. The control pulses are designed via optimization algorithms by considering both the system and environment. As stated above, the ideal pulses are not effective for the open systems. In this paper, we use Adam algorithm to design the optimized couplings or pulses for high-fidelity QST through a spin chain in a non-Markovian environment. By defining an effective loss function which is relevant to the system and environmental parameters, the real unknown parameters can be revealed and the optimized solution is obtained along the gradient descent direction. We adopt a new-developed non-Markovian quantum master equation approach to solve the corresponding dynamics of the system [28]. For the optimized couplings, we find that the achievable maximum fidelity can be enhanced and the corresponding arrival time can be shortened as well.

* wangzhaoming@ouc.edu.cn

For the optimized control pulses, our results show that they can acquire better QST qualities than the ideal closed-system pulses do. In both scenarios, the effects of system-bath coupling strength Γ , environmental non-Markovianity γ and temperature T on the fidelity are analyzed. The fidelity decreases with increasing anyone of above parameters as expected, but the fidelity can be improved by our optimized schemes, especially in a strong environment.

II. MODEL AND METHOD

A. The model and the Hamiltonian

When a quantum system is exposed to its environment, the total Hamiltonian H_{tot} consists of three parts

$$H_{tot} = H_s + H_b + H_{int}. \quad (1)$$

Here H_s and $H_b = \sum_k \omega_k b_k^\dagger b_k$ are the system and bath Hamiltonian, respectively. $H_{int} = \sum_k (g_k^* L^\dagger b_k + g_k L b_k^\dagger)$ accounts for the interaction between them. ω_k indicates the k th mode frequency of bath and b_k^\dagger (b_k) represents the bosonic creation (annihilation) operator. The system is linearly coupled to a bosonic bath through the Lindblad operator L with coupling constant g_k .

According to the QSD approach [28–31], the dynamical evolution of an open system in a non-Markovian finite-temperature heat bath is governed by

$$\begin{aligned} \frac{\partial}{\partial t} \rho_s = & -i[H_s, \rho_s] + [L, \rho_s \bar{O}_z^\dagger(t)] - [L^\dagger, \bar{O}_z(t) \rho_s] \\ & + [L^\dagger, \rho_s \bar{O}_w^\dagger(t)] - [L, \bar{O}_w(t) \rho_s]. \end{aligned} \quad (2)$$

The operators $O_{z(w)}$ are defined by an ansatz, and enter this evolution equation through the memory kernels $\bar{O}_{z(w)}(t) = \int_0^t ds \alpha_{z(w)}(t-s) O_{z(w)}(t,s)$. To simplify, we adopt the weak system-bath coupling and low frequency (or high temperature) approximations. Moreover, the chosen spectrum density, Ohmic type with a Lorentz-Drude cutoff function [32–34], reads $J(\omega) = \frac{\Gamma}{\pi} \frac{\omega}{1+(\frac{\omega}{\gamma})^2}$. Subsequently, the two bath correlation functions $\alpha_{z(w)}(t-s)$ in $\bar{O}_{z(w)}(t)$ satisfy the following condition

$$\frac{\partial \alpha_{z(w)}(t-s)}{\partial t} = -\gamma \alpha_{z(w)}(t-s). \quad (3)$$

Then the operators $\bar{O}_{z(w)}(t)$ obey the closed equations [28]

$$\frac{\partial \bar{O}_z}{\partial t} = \left(\frac{\Gamma T \gamma}{2} - \frac{i \Gamma \gamma^2}{2} \right) L - \gamma \bar{O}_z + [-i H_s - (L^\dagger \bar{O}_z + L \bar{O}_w), \bar{O}_z], \quad (4)$$

$$\frac{\partial \bar{O}_w}{\partial t} = \frac{\Gamma T \gamma}{2} L^\dagger - \gamma \bar{O}_w + [-i H_s - (L^\dagger \bar{O}_z + L \bar{O}_w), \bar{O}_w]. \quad (5)$$

As a result, we are allowed to numerically solve the dynamical evolution equation in Eq. (2), with the help of Eqs. (4) and (5). In the above derivation, Γ and γ stand for the system-bath coupling strength and the characteristic frequency of bath. The Ornstein-Uhlenbeck correlation function $\Lambda(t,s) = \frac{\gamma}{2} e^{-\gamma|t-s|}$ contained in $\alpha_{z(w)}(t-s)$, decays exponentially with the environmental memory time $1/\gamma$ characterizing the memory capacity of the bath. Therefore for small γ , non-Markovian properties can be observed. The large γ corresponds to a Markovian bath due to the shrinking environmental memory time.

When γ approaches ∞ , the bath becomes completely Markovian and has no memory capacity anymore. Consequently, $\bar{O}_z = \frac{\Gamma T}{2} L$ and $\bar{O}_w = \frac{\Gamma T}{2} L^\dagger$. The master equation in Eq. (2) therefore reduces to the Lindblad form [28]

$$\begin{aligned} \frac{\partial}{\partial t} \rho_s = & -i[H_s, \rho_s] + \frac{\Gamma T}{2} [(2L \rho_s L^\dagger - L^\dagger L \rho_s - \rho_s L^\dagger L) \\ & + (2L^\dagger \rho_s L - L L^\dagger \rho_s - \rho_s L L^\dagger)]. \end{aligned} \quad (6)$$

In this paper, we consider a one-dimensional XY spin chain as the system

$$H_s = \sum_{i=1}^{N-1} J_{i,i+1} (\sigma_i^x \sigma_{i+1}^x + \sigma_i^y \sigma_{i+1}^y). \quad (7)$$

Here σ_i^α ($\alpha = x, y$) stands for the Pauli operator acting on the i th spin. $J_{i,i+1}$ indicates the relevant coupling strength between the nearest-neighbor sites $i, i+1$ and we set the PST coupling layout $J_{i,i+1} = -\sqrt{i(N-i)}$ throughout.

Initially prepare all the spins at the down state but the first one at the up state, i.e., $|\Psi_s(0)\rangle = |1\rangle = |100\dots 0\rangle$. Our task is to transfer the state $|1\rangle$ from the first to the last spin of the chain, and the target state will be $|\mathbf{N}\rangle = |000\dots 1\rangle$. During this process, the transmission fidelity $F(t) = \sqrt{\langle \mathbf{N} | \rho_s(t) | \mathbf{N} \rangle}$ is monitored to evaluate the transfer quality. Here $\rho_s(t)$ is the reduced density matrix of our system.

Combining the advantages of two algorithms with fast and steady convergence, Momentum and RMSprop, Adam has already become the most valuable optimizer in the NISQ era. Now in this work we use the Adam to construct an iterative process to optimize the parameters for high-fidelity state transfer in noisy environments.

First we need to define a loss function $Loss$ and our goal of high-fidelity QST is encoded as to minimize the $Loss$. The specific optimization procedure of Adam algorithm is as follows.

Step 1: Compute the gradient vector \mathbf{g} of loss function $Loss$ with respect to selected variables \mathbf{A} in the k th iteration

$$\mathbf{g}^k = \nabla_{\mathbf{A}^k} Loss(\mathbf{A}^k). \quad (8)$$

Step 2: Compute the new exponential moving averages

$$\mathbf{m}^k = \beta_1 \mathbf{m}^{k-1} + (1 - \beta_1) \mathbf{g}^k, \quad (9)$$

$$\mathbf{v}^k = \beta_2 \mathbf{v}^{k-1} + (1 - \beta_2)(\mathbf{g}^k)^2. \quad (10)$$

Step 3: Compute the new bias-corrected moment vectors

$$\hat{\mathbf{m}}^k = \mathbf{m}^k / [1 - (\beta_1)^k], \quad (11)$$

$$\hat{\mathbf{v}}^k = \mathbf{v}^k / [1 - (\beta_2)^k]. \quad (12)$$

Step 4: Update the variables \mathbf{A} according to

$$\mathbf{A}^{k+1} = \mathbf{A}^k - \alpha \hat{\mathbf{m}}^k / (\sqrt{\hat{\mathbf{v}}^k} + \varepsilon). \quad (13)$$

Step 5: Repeat steps 1 – 4 till $Loss < \xi$ or the number of iterations $k > k_{max}$. ξ (set $\xi = 0.001$) and k_{max} are the prescribed loss ceiling and maximal iteration number, respectively.

III. RESULTS AND DISCUSSIONS

In this work, we consider two scenarios and apply Adam optimizer to explore high-fidelity QST through a spin chain in open systems. For the first one, we choose to modulate the coupling strength sequence $\mathbf{J} = [J_{1,2}, J_{2,3}, \dots, J_{N-1,N}]$. For the second one, we optimize the pulse amplitude sequence $\mathbf{I} = [I_0, I_1, \dots, I_{M-1}]$ to realize a more effective LEO. Without loss of generality, we consider the Lindblad operator $L = \sum_{i=1}^N \sigma_i^-$ that describes the dissipation. Here $\sigma_i^- = (\sigma_i^x - i\sigma_i^y)/2$ denotes the lowering operator on the i th spin.

A. Optimized couplings via Adam

In this section, we perform the coupling optimization. Recall that our goal is to minimize a commonly defined loss function

$$Loss(\mathbf{J}) = 1 - F(\mathbf{J}) + \lambda J_{max}, \quad (14)$$

where the fidelity $F(\mathbf{J})$ is obtained with the help of the optimized coupling sequence \mathbf{J} and $Loss(\mathbf{J})$ is the corresponding infidelity. J_{max} stands for the maximal absolute value of couplings $J_{i,i+1}$ in optimized couplings. The relaxation parameter λ is introduced here to modulate the proportion of J_{max} in $Loss$ to restrain J_{max} to not too large.

As an example, the number of spins is taken as $N = 6$. Here we take the PST couplings $J_{i,i+1} = -\sqrt{i(N-i)}$ as an initial guess and set the maximal iteration number $k_{max} = 1000$. In addition, it is necessary to mention that in closed systems, PST can be observed at $t = n\pi/4$ (n is an odd integer) for the PST couplings. Accordingly, the total evolution time is taken as $T_{tot} = \pi/4$ throughout.

In Fig. 1 we plot the time evolution of the fidelity $F(t/T_{tot})$ with PST and optimized couplings for different

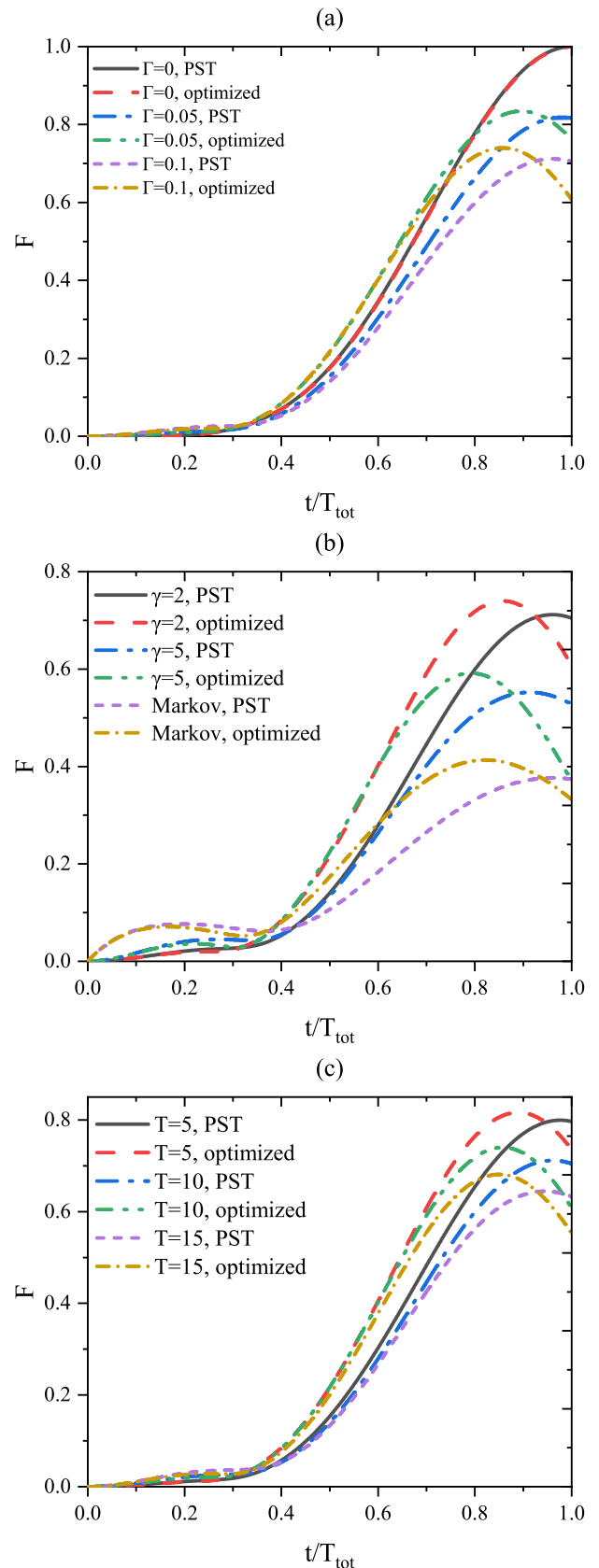


FIG. 1. (Color on line) The fidelity F versus the rescaled time t/T_{tot} with PST and optimized couplings for different parameters (a) Γ , $\gamma = 2$, $T = 10$; (b) γ , $\Gamma = 0.1$, $T = 10$; (c) T , $\Gamma = 0.1$, $\gamma = 2$. $N = 6$, $L = \sum_{i=1}^N \sigma_i^-$.

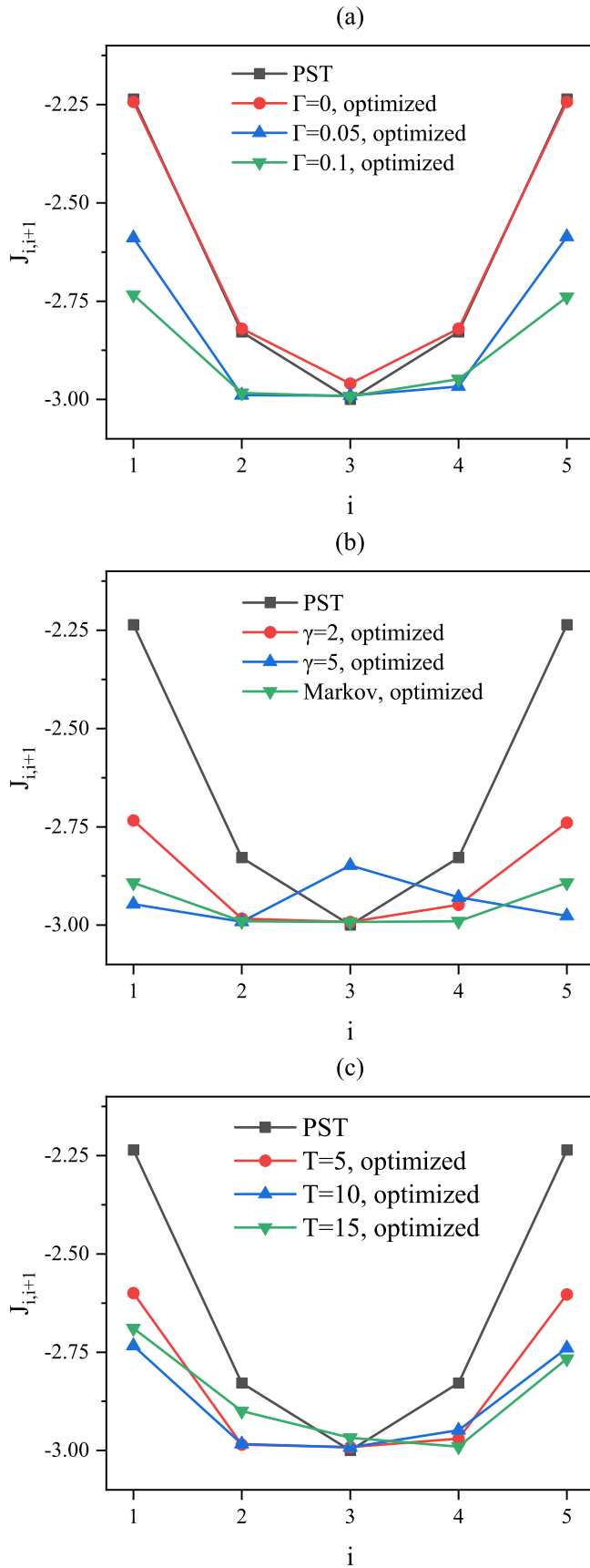


FIG. 2. (Color on line) The corresponding PST and optimized couplings in Fig. 1.

environmental parameters. The parameters are taken as $\gamma = 2$, $T = 10$ (Fig. 1(a)), $\Gamma = 0.01$, $T = 10$ (Fig. 1(b)), and $\Gamma = 0.01$, $\gamma = 2$ (Fig. 1(c)), respectively. For a fair comparison between PST and optimized couplings, the optimized couplings are limited in $[-3, -2]$, which has the same region as PST. At first, without optimization, the exposure to environment always decreases the fidelity. A larger Γ , γ or T corresponds to a lower fidelity F , i.e., a stronger system-bath interaction, more Markovian or higher temperature bath will destroy the system more severely, which is in accordance with Refs. [16, 18]. This result still holds for the optimized cases. For example, in Fig. 1(b), the maximum fidelity $F_{max} = 0.73$ is obtained for $\gamma = 2$ and as γ grows, F_{max} decreases. Secondly, comparing F_{max} for the PST and optimized couplings with the same environmental parameters, we find that the optimized F_{max} are always higher than these in the ideal cases. In another word, using the optimized couplings, F_{max} can always be enhanced in the presence of environment. This is the key observation of our paper. It is not so obvious but worth mentioning that the maximal fidelity improvement increases with increasing Γ and T . That is to say, the bath destroys system more severely, the improvement is more significant. Namely, a more stronger bath provides more space for Adam to optimize. Clearly, without environment ($\Gamma = 0$ in Fig. 1(a)), the evolution is the same for PST and optimized couplings. Thirdly, defining the arrival time T_a when F_{max} is achieved, with PST couplings, T_a occurs at $t = \pi/4$ for different Γ and T , and nearly at $t = \pi/4$ for different γ . The bath slightly affects the arrival time T_a under ideal pulses. However, after optimization, T_a is evidently shorter than $\pi/4$, which bears the advantage that F_{max} arrives earlier and thus the accumulative detrimental effects of the environment can be partially avoided. In Fig. 1, T_a is shorter for larger Γ , γ and T . At last, even for the Markovian case (Fig. 1(b)), F_{max} can still be enhanced by the coupling optimization. In sum, our optimized couplings via Adam algorithm can simultaneously enhance the transmission fidelity and shorten the arrival time.

Fig. 2 plots the corresponding PST and optimized couplings used in Fig. 1. The optimized coupling configuration is similar to the PST: bigger in the middle and smaller in both ends. But for a more stronger bath (bigger Γ , γ and T), Adam finds a more flatter configuration. The minimum and maximum get closer. Also, the symmetry of the couplings with respect to the middle of the chain is broken due to the existence of the environments, which can be clearly seen for a strong bath ($\Gamma = 0.1$ in Fig. 2(a), $\gamma = 5$ in Fig. 2(b), or $T = 15$ in Fig. 2(c)).

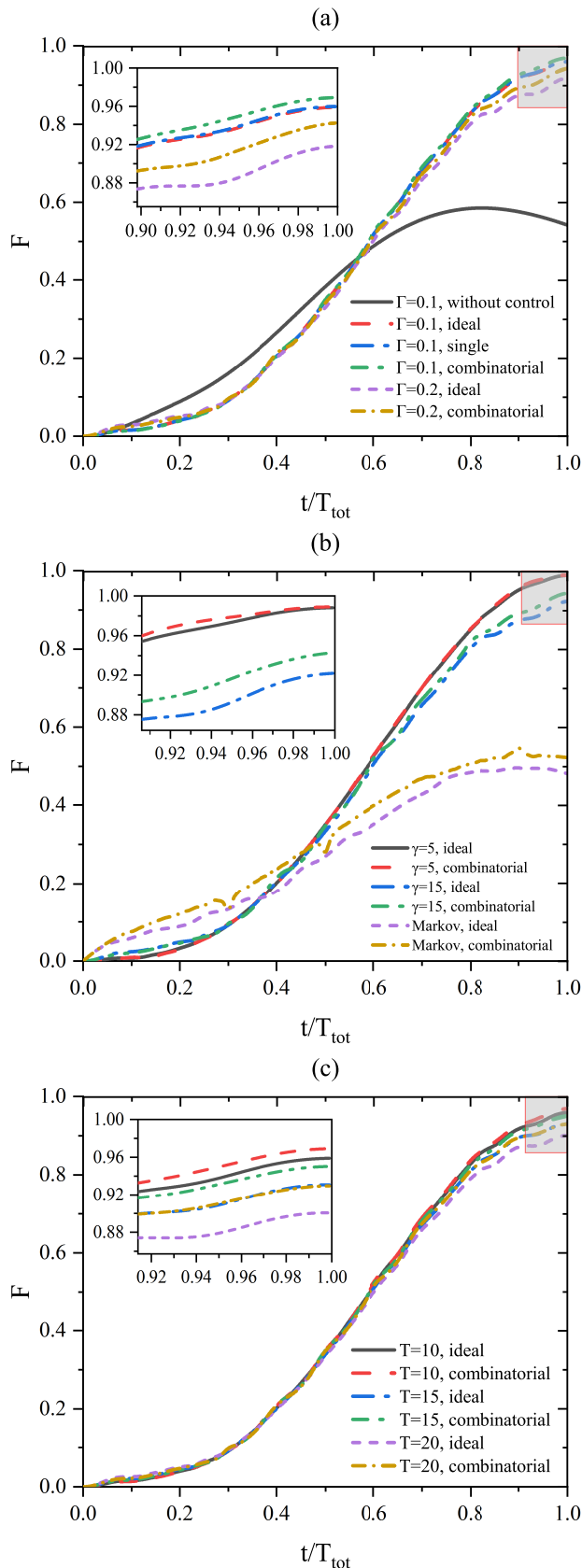


FIG. 3. (Color on line) The fidelity F versus the rescaled time t/T_{tot} with ideal and optimized (single and combinatorial) pulses for different parameters (a) $\Gamma, \gamma = 10, T = 10$; (b) $\gamma, \Gamma = 0.1, T = 10$; (c) $T, \Gamma = 0.1, \gamma = 10$.

B. Optimized pulses via Adam

1. QST under ideal pulse control

Environmental noise normally destroy the transmission fidelity and Refs. [18, 28] have introduced an LEO approach to address this problem. The main idea of this LEO approach is to add an additional Hamiltonian H_{LEO} to the system Hamiltonian H_s , ensuring the quantum system to evolve along a predefined passage. For example, if we use H_{PST} to denote the Hamiltonian in Eq. (7) with PST couplings, we can set $|\Psi(t)\rangle = \exp(-iH_{PST}t)|1\rangle$ as the evolution passage. The LEO Hamiltonian in adiabatic frame [35] can be constructed as

$$H_{LEO} = c(t)|\Psi(t)\rangle\langle\Psi(t)|, \quad (15)$$

where $c(t)$ is the control function. The total Hamiltonian becomes

$$H_{tot} = H_s + H_{LEO}. \quad (16)$$

The LEO Hamiltonian can be achieved by a series of control pulses that can be divided into perturbative and nonperturbative versions. In this paper we consider the latter one whose pulse intensity and duration are finite. The pulse conditions for effective control have been theoretically deduced by P-Q partitioning technique in closed systems [19, 36, 37]. For sine pulses $c(t) = I \sin(\omega t)$, the corresponding pulse condition is

$$J_0\left(\frac{I\tau}{\pi}\right) = 0. \quad (17)$$

Here I and τ represent pulse intensity and half period, and $J_0(x)$ denotes the zero-order Bessel function of the first kind. Note that the integral of such pulses over a period is zero (i.e., zero-area condition of pulses) [19, 35]. The control pulses such as rectangular and triangular ones have also been investigated [37].

2. High-fidelity QST

Although the above ideal pulse conditions are derived theoretically from closed systems, they can be applied to open ones with no guarantee of their effectiveness. In this section, we aim to design optimized pulses for certain environmental parameters with the help of Adam, and then compare their performances with ideal counterparts. In order to make fair comparisons, the optimized pulses also satisfy the zero-area condition [19, 35]. First we design the optimized sine pulses (single pulses)

$$c(t) = I(t) \sin(\omega t). \quad (18)$$

Here $I(t)$ is a P segment piece-wise constant function, whose P values are drawn in order from the pulse

amplitude sequence $\mathbf{I} = [I_0, I_1, \dots, I_{P-1}]$ and take the equal time interval $\Delta t = T_{tot}/P$ ($\omega = 2\pi/\Delta t$ and set $P = 5$). Notice that the zero-area condition [19, 35] is followed in iterative procedures as in theoretical derivation. We consider the corresponding ideal values $\mathbf{I} = [96.200, 96.200, \dots, 96.200]$, derived from the pulse condition in Eq. (17), as our initial guess. The maximal iteration number is still $k_{max} = 1000$ and the number of spins $N = 4$. Furthermore, the maximal intensity of the optimized pulses are not supposed to outweigh that of their ideal counterparts. Similar to Eq. (14), the loss function is accordingly defined as

$$Loss(\mathbf{I}) = 1 - F(\mathbf{I}) + \lambda c_{max}. \quad (19)$$

Here c_{max} is the maximum of the control function $c(t)$. In Eq. (19), there also is a competition between infidelity $1 - F(\mathbf{I})$ and maximal control intensity c_{max} for $Loss$, and a relaxation parameter λ to restrict c_{max} [38].

In Fig. 3, we plot the fidelity F as a function of the rescaled time t/T_{tot} for different environmental parameters with ideal and optimized pulses. In Fig. 3(a), $\gamma = 10$ and $T = 10$. When $\Gamma = 0.1$, the maximal fidelity $F_{max}(t)$ dramatically rockets, from 0.585 without control to 0.958 with ideal pulses and 0.959 with single pulses. Note that the single pulses ultimately reach the similar fidelities as the ideal pulses can do. We then propose the combinatorial sine pulses (combinatorial pulses) to obtain a higher fidelity,

$$c(t) = \sum_{i=0}^{Q-1} I_i \sin[(i+1)\omega t], \quad (20)$$

where we turn to set the control function $c(t)$ as a combination of Fourier sine components. Here Q denotes the number of Fourier components and we consider $Q = 10$. Notice that the zero-area condition [19, 35] is still satisfied. Obviously, when $\Gamma = 0.1$ and 0.2, combinatorial pulses overshadow the ideal and single counterparts, and there are minor but evident increases on QST fidelities. From now on, we choose to optimize combinatorial pulses alone.

In Fig. 3(b) and (c), we plot the influences of the parameters γ and temperature T on the fidelity. In Fig. 3(b), $\Gamma = 0.1$ and $T = 10$ while in Fig. 3(c), $\Gamma = 0.1$ and $\gamma = 10$. For all the situations, without exception, the combinatorial pulses outshine the ideal ones. Furthermore, an increasing Γ , γ or T corresponds to a decreasing fidelity F . But still, in a more stronger bath, the optimized pulses can make larger corrections for this fidelity deterioration. Fig. 4 gives the profiles of corresponding ideal and optimized (single and combinatorial) pulses in Fig. 3. Fig. 4(a) shows that the single pulses are almost indistinguishable from the ideal ones. As for the combinatorial pulses, they are only similar with the ideal pulses in terms of the magnitude. From the above analysis, we conclude that the scheme of optimized control pulses can play more helpful roles than the ideal ones, especially in stronger baths.

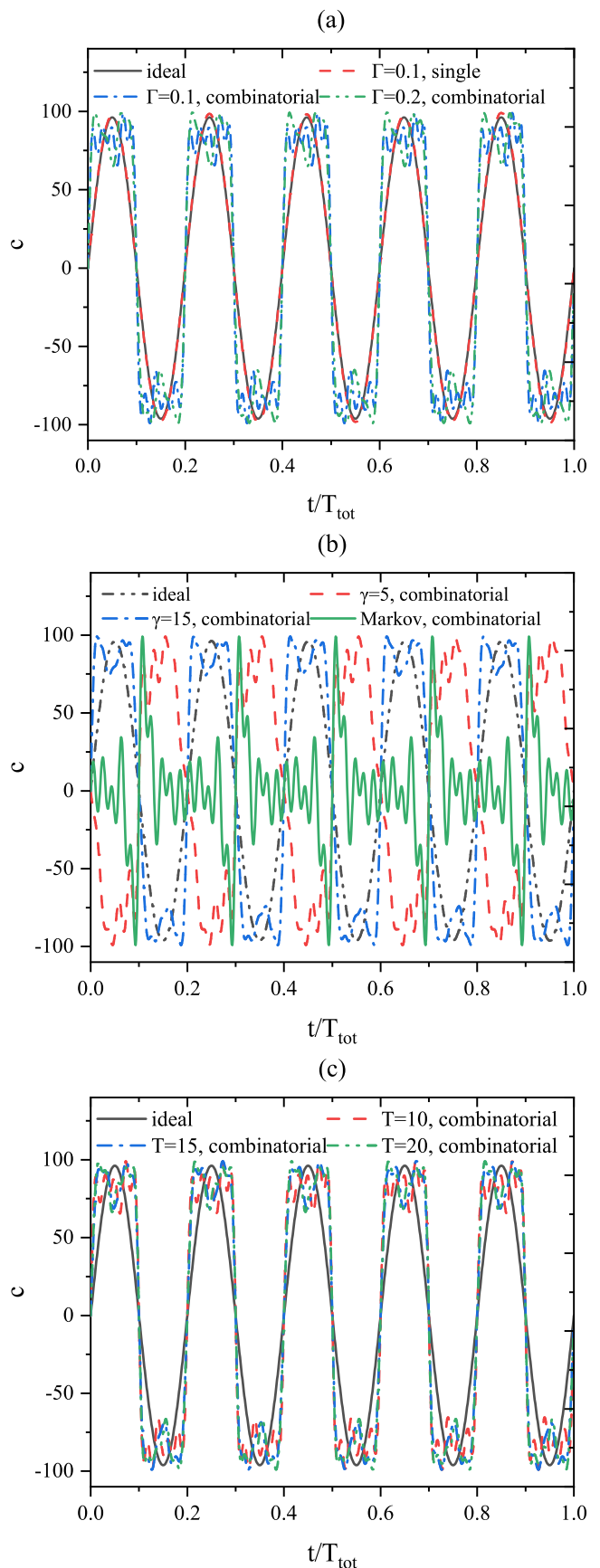


FIG. 4. (Color on line) The corresponding ideal and optimized (single and combinatorial) pulses in Fig. 3.

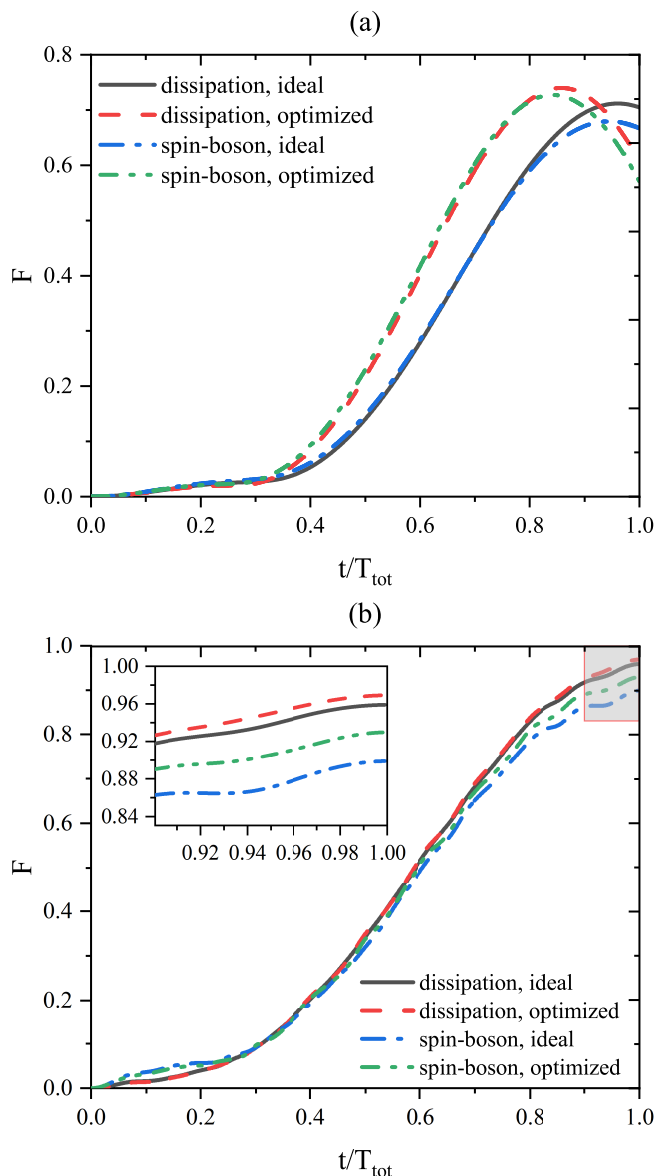


FIG. 5. (Color on line) The fidelity F versus the rescaled time t/T_{tot} for different Lindblad operators $L = \sum_{i=1}^N \sigma_i^x$ and $L = \sum_{i=1}^N \sigma_i^-$ with (a) PST and optimized couplings; (b) ideal and optimized (combinatorial) pulses. $T = 10$. $N = 6$, $\Gamma = 0.05$ and $\gamma = 2$ in Fig. 5(a). $N = 4$, $\Gamma = 0.1$ and $\gamma = 10$ in Fig. 5(b).

At last we consider different types of Lindblad operator L . We will compare the effects of $L = \sum_{i=1}^N \sigma_i^-$ and

$L = \sum_{i=1}^N \sigma_i^x$, and the latter corresponds to the spin-boson interaction. We do not consider the dephasing ($L = \sum_{i=1}^N \sigma_i^z$) because $[L, \rho_s \bar{\mathcal{O}}^\dagger] = [L^\dagger, \bar{\mathcal{O}} \rho_s] = 0$. Therefore the bath only randomly changes the global phase of system [9]. In Fig. 5 we plot the cases with different Lindblad operators. Fig. 5(a) shows that the fidelity obtained by the optimized couplings exceeds the PST ones whatever the Lindblad operator L is. The parameters are taken as $N = 6$, $\Gamma = 0.05$, $\gamma = 2$ and $T = 10$. Fig. 5(b) demonstrates the implications of L on performances of optimized pulses. Again optimized pulses show their advantage over the ideal counterparts on reducing the effects of environmental noise. We take $N = 4$, $\Gamma = 0.1$, $\gamma = 10$ and $T = 10$ in the simulation.

IV. CONCLUSIONS

QST is one of the basic tasks in quantum computation. PST and almost exact QST through a spin chain can be realized for PST couplings and LEO control, respectively. However, these conditions are derived theoretically from the ideally closed systems and thus their effectiveness are lost when they are applied to an open system, i.e., being coupled to a heat bath results in their dissipation dynamics. In this paper, we take a one-dimensional XY spin chain with nearest-neighbor couplings as an example and introduce a well-developed optimization algorithm, Adam, to seek for the optimized couplings and control pulses in the presence of environment. By minimizing a predefined loss function, high-fidelity transmission is obtained for both schemes. In addition, we discuss the effects of system-bath coupling strength Γ , environmental non-Markovianity parameter γ and temperature T on our schemes. Although the fidelity F decreases with anyone of these parameters increasing, our optimized schemes perform better, especially for a stronger bath. Our work shows that the Adam algorithm is a powerful tool to search the optimized parameters in open quantum systems, which are important in performing quantum information processing tasks.

ACKNOWLEDGMENT

This paper is based upon work supported by the Natural Science Foundation of Shandong Province (Grants No. ZR2021LLZ004).

[1] H. J. Kimble, The quantum internet, *Nature* **453**, 1023 (2008).
 [2] S. Bose, Quantum communication through an unmodulated spin chain, *Physical review letters* **91**, 207901 (2003).

[3] M.-L. Hu and H.-L. Lian, State transfer in intrinsic decoherence spin channels, *The European Physical Journal D* **55**, 711 (2009).
 [4] M. Christandl, N. Datta, A. Ekert, and A. J. Landahl, Perfect state transfer in quantum spin networks,

- Phys. Rev. Lett. **92**, 187902 (2004).
- [5] M. Christandl, N. Datta, T. C. Dorlas, A. Ekert, A. Kay, and A. J. Landahl, Perfect transfer of arbitrary states in quantum spin networks, *Physical Review A* **71**, 032312 (2005).
- [6] J. Fitzsimons and J. Twamley, Globally controlled quantum wires for perfect qubit transport, mirroring, and computing, *Physical review letters* **97**, 090502 (2006).
- [7] V. Balachandran and J. Gong, Adiabatic quantum transport in a spin chain with a moving potential, *Physical Review A* **77**, 012303 (2008).
- [8] M. Murphy, S. Montangero, V. Giovannetti, and T. Calarco, Communication at the quantum speed limit along a spin chain, *Phys. Rev. A* **82**, 022318 (2010).
- [9] Z.-M. Wang, F.-H. Ren, D.-W. Luo, Z.-Y. Yan, and L.-A. Wu, Almost-exact state transfer by leakage-elimination-operator control in a non-markovian environment, *Physical Review A* **102**, 042406 (2020).
- [10] X. Li, Y. Ma, J. Han, T. Chen, Y. Xu, W. Cai, H. Wang, Y. Song, Z.-Y. Xue, Z.-q. Yin, *et al.*, Perfect quantum state transfer in a superconducting qubit chain with parametrically tunable couplings, *Physical Review Applied* **10**, 054009 (2018).
- [11] J. Zeiher, J.-y. Choi, A. Rubio-Abadal, T. Pohl, R. Van Bijnen, I. Bloch, and C. Gross, Coherent many-body spin dynamics in a long-range interacting ising chain, *Physical review X* **7**, 041063 (2017).
- [12] F. Grusdt, T. Li, I. Bloch, and E. Demler, Tunable spin-orbit coupling for ultracold atoms in two-dimensional optical lattices, *Physical Review A* **95**, 063617 (2017).
- [13] M. Veldhorst, C. Yang, J. Hwang, W. Huang, J. Dehollain, J. Muhonen, S. Simmons, A. Laucht, F. Hudson, K. M. Itoh, *et al.*, A two-qubit logic gate in silicon, *Nature* **526**, 410 (2015).
- [14] Y. P. Kandel, H. Qiao, S. Fallahi, G. C. Gardner, M. J. Manfra, and J. M. Nichol, Adiabatic quantum state transfer in a semiconductor quantum-dot spin chain, *Nature communications* **12**, 2156 (2021).
- [15] A. Ablimit, R.-H. He, Y.-Y. Xie, L.-A. Wu, and Z.-M. Wang, Quantum energy current induced coherence in a spin chain under non-markovian environments, *Entropy* **24**, 1406 (2022).
- [16] Z.-M. Wang, M. S. Sarandy, and L.-A. Wu, Almost exact state transfer in a spin chain via pulse control, *Physical Review A* **102**, 022601 (2020).
- [17] J. Jeske, N. Vogt, and J. H. Cole, Excitation and state transfer through spin chains in the presence of spatially correlated noise, *Physical Review A* **88**, 062333 (2013).
- [18] S.-S. Nie, F.-H. Ren, R.-H. He, J. Wu, and Z.-M. Wang, Control cost and quantum speed limit time in controlled almost-exact state transmission in open systems, *Physical Review A* **104**, 052424 (2021).
- [19] R.-H. He, R. Wang, F.-H. Ren, L.-C. Zhang, and Z.-M. Wang, Adiabatic speedup in cutting a spin chain via zero-area pulse control, *Physical Review A* **103**, 052606 (2021).
- [20] X.-M. Zhang, Z. Wei, R. Asad, X.-C. Yang, and X. Wang, When does reinforcement learning stand out in quantum control? a comparative study on state preparation, *npj Quantum Information* **5**, 85 (2019).
- [21] I. Sutskever, J. Martens, G. Dahl, and G. Hinton, On the importance of initialization and momentum in deep learning, in *International conference on machine learning* (PMLR, 2013) pp. 1139–1147.
- [22] T. Kurbiel and S. Khaleghian, Training of deep neural networks based on distance measures using rmsprop, arXiv preprint arXiv:1708.01911 (2017).
- [23] D. P. Kingma and J. Ba, Adam: A method for stochastic optimization, arXiv preprint arXiv:1412.6980 (2014).
- [24] S. J. Reddi, S. Kale, and S. Kumar, On the convergence of adam and beyond, arXiv preprint arXiv:1904.09237 (2019).
- [25] R.-H. He, X.-S. Xu, M. Byrd, and Z.-M. Wang, Modularized and scalable compilation for double quantum dot quantum computing, (2023).
- [26] Y.-Y. Xie, F.-H. Ren, R.-H. He, A. Ablimit, and Z.-M. Wang, Stochastic learning control of adiabatic speedup in a non-markovian open qutrit system, *Phys. Rev. A* **106**, 062612 (2022).
- [27] X.-H. Liang, L.-A. Wu, and Z.-M. Wang, Optimally controlled non-adiabatic quantum state transmission in the presence of quantum noise, in *Photonics*, Vol. 10 (MDPI, 2023) p. 274.
- [28] Z.-M. Wang, F.-H. Ren, D.-W. Luo, Z.-Y. Yan, and L.-A. Wu, Quantum state transmission through a spin chain in finite-temperature heat baths, *Journal of Physics A: Mathematical and Theoretical* **54**, 155303 (2021).
- [29] T. Yu, L. Diósi, N. Gisin, and W. T. Strunz, Non-markovian quantum-state diffusion: Perturbation approach, *Physical Review A* **60**, 91 (1999).
- [30] T. Yu, Non-markovian quantum trajectories versus master equations: Finite-temperature heat bath, *Physical Review A* **69**, 062107 (2004).
- [31] L. Diósi, N. Gisin, and W. T. Strunz, Non-markovian quantum state diffusion, *Physical Review A* **58**, 1699 (1998).
- [32] H. Wang and M. Thoss, From coherent motion to localization: II. dynamics of the spin-boson model with sub-ohmic spectral density at zero temperature, *Chemical Physics* **370**, 78 (2010).
- [33] G. Ritschel and A. Eisfeld, Analytic representations of bath correlation functions for ohmic and superohmic spectral densities using simple poles, *The Journal of chemical physics* **141**, 094101 (2014).
- [34] C. Meier and D. J. Tannor, Non-markovian evolution of the density operator in the presence of strong laser fields, *The Journal of chemical physics* **111**, 3365 (1999).
- [35] Z.-M. Wang, M. S. Byrd, J. Jing, and L.-A. Wu, Adiabatic leakage elimination operator in an experimental framework, *Physical Review A* **97**, 062312 (2018).
- [36] Y. Chen, L. Zhang, Y. Gu, and Z.-M. Wang, Acceleration of adiabatic quantum state transfer in a spin chain under zero-energy-change pulse control, *Physics Letters A* **382**, 2795 (2018).
- [37] L.-C. Zhang, F.-H. Ren, Y.-F. Chen, R.-H. He, Y.-J. Gu, and Z.-M. Wang, Adiabatic speedup via zero-energy-change control in a spin system, *Europhysics Letters* **125**, 10010 (2019).
- [38] X.-M. Zhang, Z.-W. Cui, X. Wang, and M.-H. Yung, Automatic spin-chain learning to explore the quantum speed limit, *Physical Review A* **97**, 052333 (2018).